Polymer Bulletin (2021) 78:313–334
https://doi.org/10.1007/s00289-020-03110-w

ORIGINAL PAPER

Cross-linking network structures and mechanical properties of novel HTPE/PCL binder for solid propellant

Shen Yuan[1,2] · Shengkun Jiang[1,2] · Yunjun Luo[1,2]

Received: 4 September 2019 / Revised: 23 December 2019 / Accepted: 14 January 2020 /
Published online: 22 January 2020

Abstract

A series of cross-linked hydroxyl-terminated polyether and poly(ε-caprolactone) HTPE/PCL binders were prepared by varying the relative mass contents of PCL to HTPE. The correlations between the microstructures and macroscopic mechanical properties of HTPE/PCL binders at a wide temperature range of − 50 to 70 °C were investigated. The cross-linking network structures of HTPE/PCL binders were analyzed by Fourier transform infrared spectroscopy (FT-IR), X-ray diffraction (XRD) and low-field nuclear magnetic resonance (LF-NMR), and the universal testing machine was used to characterize the mechanical properties of HTPE/PCL binders. It is found that the influence of adding PCL on the physical cross-linking network structures is not obvious, but it reduces the degree of microphase separation. For the chemical cross-linking network structures of HTPE/PCL binders, the cross-linking density (V_e) demonstrates an increasing tendency with enhancing PCL mass content, but the molecular weight between the cross-linking points (M_c) shows an opposite change trend. The addition of PCL can improve the maximum tensile strength (σ_m) of HTPE/PCL binders under the wide temperature range of − 50 to 70 °C. The HTPE/PCL binder with 40 wt% PCL possesses the better mechanical properties; its σ_m increases from 0.63 to 0.81 MPa at 20 °C, 1.64 to 3.06 MPa at − 50 °C and 0.57 to 0.68 MPa at 70 °C separately comparing with the HTPE binder.

Keywords Hydroxyl-terminated polyether (HTPE) · Poly(ε-caprolactone) (PCL) · Cross-linking network structure · Mechanical property · Wide temperature range

Electronic supplementary material The online version of this article (https://doi.org/10.1007/s00289-020-03110-w) contains supplementary material, which is available to authorized users.

✉ Yunjun Luo
yjluo@bit.edu.cn

[1] School of Materials Science and Engineering, Beijing Institute of Technology, Beijing 100081, China

[2] Key Laboratory for Ministry of Education of High Energy Density Materials, Beijing Institute of Technology, Beijing 100081, China

Introduction

In order to ensure the normal operation of the solid rocket motor, the solid propellant should have the mechanical property that can bear various loads without being destroyed during the temperature range of its processing, use and storage [1]. The mechanical property of the solid propellant is one of its most important physical properties [2–4]. The mechanical property of the solid propellant is mainly affected by its binder with a mass fraction of 10–20% [1]. The cross-linking network-structured polyurethane is a highly effective binder [5–7]. The cross-linking structure of polyurethane network, which can be formed by the reaction of prepolymer and isocyanate, is one of the key factors to the mechanical property of binder [8]. The cross-linking network structure of binder includes chemical and physical cross-linking network structures. The cross-linking density (V_e) and the molecular weight between the cross-linking points (M_c) are the characteristic parameters of chemical cross-linking network structure [9]. And the physical cross-linking network structure can be determined by intermolecular interactions, such as the hydrogen bonded (H-bonded) interaction and the intermolecular interaction caused by crystallization. It is commonly believed that the H-bonded interaction formed through the urethane hard segments and intermolecular interaction caused by crystallization are the mainly driving forces for the formation of microphase separation in polyurethane binder, which gives rise to the favorable mechanical property [10–12]. Thus, the study of the cross-linking network structure and mechanical property of the polyurethane binder is one of the criteria for evaluating its suitability for the application in solid propellants [9]. Yarmohammadi et al. [13] investigated the effect of different cross-linking structures on the mechanical properties of hydroxyl-terminated polybutadiene (HTPB) polyurethanes. The result shows that HTPB polyurethane with T313 (boron trifluoride triethanolamine complex) as the cross-linker agent led to increasing chemical cross-linking bonds in comparison with TEA (triethanolamine) and TMP (trimethylolpropane). Ou et al. [14] compared the effects of linear and cross-linking structures on the mechanical properties of HTPB polyurethanes, and the cross-linking HTPB polyurethane possesses better mechanical properties than the linear one.

Hydroxyl-terminated polyether (HTPE) is a new type of polyurethane binder with high performances, in which the ether bonds give it good flexibility [15]. HTPE binder can obtain favorable low-temperature mechanical property and good compatibility with energetic nitrate plasticizers [16, 17]. HTPE binder can meet the requirements of insensitive munition (IM) properties. Using HTPE binder can reduce the solid content of solid propellant, and HTPE binder itself has a higher dielectric coefficient of electrostatic insulation comparing with HTPB binder. Hence, it can improve the IM properties of HTPE propellant such as shock wave, mechanical impact and electrostatic ignition, and meanwhile weaken the response of slow cook-off [18–23]. Mao et al. [24] studied the effect of different curing agents on the cross-linking point structures and mechanical properties; it reveals that the mechanical properties of HTPE binder can be improved by using the toluene diisocyanate (TDI) and the polyfunctional isocyanate (N-100) as the compound curing agent. With the

diversification and deepening of various tasks, and the increasing demand for high- and low-temperature extreme conditions, it is required that the HTPE binder should have better mechanical properties in order to withstand the different loads generated over a wide temperature range of − 50 to 70 °C and ensure the safety of the solid rocket motor [25–27]. However, the relationship between H-bonded interactions and temperature is very close. The high temperature makes the H-bonded interactions weak [28]. Besides, the low temperature also limits the activity of the molecular chains in HTPE binder. These reasons make HTPE binder unable to implement the requirements of mechanical properties in the wide temperature range. Hence, it is meaningful to improve the high- and low-temperature mechanical properties of HTPE-based binder.

Poly(ε-caprolactone) (PCL) is a semicrystalline aliphatic polyester formed by ring-opening polymerization of caprolactone, which has a linear molecular chain with regular arrangement and good flexibility [29, 30]. PCL has exhibited higher strain capability using the binder in solid propellant for special application [31]. It is sufficiently proven that the introduction of linear and flexible PCL into a polyurethane binder can enhance the mechanical properties of the modified binder [32]. Unfortunately, there is almost no publicly available information on the details about PCL modifying HTPE binders.

In this work, PCL was incorporated into HTPE binder to improve the mechanical properties by forming block copolymer polyurethane cross-linking network structures. We focused on the correlation between the mechanical properties and cross-linking network structures of HTPE/PCL binders, and the mechanical properties under the wide temperature range of − 50 to 70 °C were also be investigated. The crucial mechanical properties and cross-linking network structures of HTPE/PCL binders were optimized by changing the mass ratios of these two prepolymers.

Materials and methods

Materials

Hydroxyl-terminated polyether (HTPE) prepolymer with the average molecular weight of 3190 g mol^{-1} and the hydroxyl group content of 0.63 mmol g^{-1}, and *N*-Butyl-*N*-(2-nitroxyethyl)nitramine (Bu-NENA) as the plasticizer were both purchased from Liming Research Institute of Chemical Industry, Henan, China. Poly(ε-caprolactone) (PCL) prepolymer with the average molecular weight of 2000 g mol^{-1} and the hydroxyl group content of 1.00 mmol g^{-1} was purchased from BASF, Germany. The chemical structures of the HTPE and PCL prepolymers are shown in Scheme 1. The curing agent polyfunctional isocyanate (N-100) with an isocyanate group content of 5.37 mmol g^{-1} was purchased from Liming Research Institute of Chemical Industry, Henan, China. The curing catalysts triphenylbismuth (TPB, 0.5%) and dibutyltin dilaurate (DBTDL, 0.5%) were, respectively, dissolved in dioctyl sebacate (DOS); these reagents were purchased from Beijing Chemical Works. HTPE, PCL and Bu-NENA were dried in vacuum for 2 days at 60 °C before use.

Scheme 1 The chemical structures of the HTPE and PCL

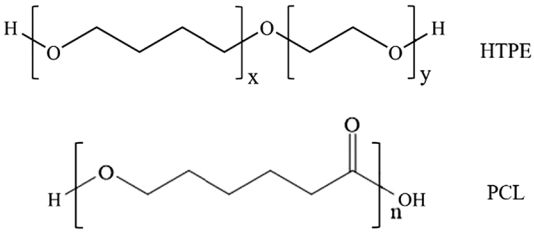

Preparation of HTPE/PCL binders

The curing parameter *R* value denotes the equivalent ratio of isocyanate (–NCO) to hydroxyl (–OH) groups, which was set to 1.7. HTPE, PCL, Bu-NENA and N-100 were weighted accurately and then stirred in an appropriate beaker. After thoroughly mixing, a 0.3 wt% solution of the mixed curing catalyst DBTDL/TPB (optimal mixing mass ratio of 1:2) was added into the beaker and continuously stirred for another 20 min. And then, the mixture was cast into a polytetrafluoroethylene mold to form a film of approximately 2–3 mm thickness. The mixture was vacuumized for 2 h under 40 °C so as to remove the residual bubbles and moisture. Subsequently, the HTPE/PCL binder was cured at 60 °C for 7 days. In this work, the HTPE/PCL binders with different PCL mass contents varying from 0 to 100 wt% were prepared by replacing HTPE with PCL equivalently.

Measurements

The hydrogen bonding (H-bonded) interactions and microphase separations were conducted using Fourier transform infrared spectroscopy (FT-IR, Nicolet 8700, Thermo Fisher Scientific, USA) with the spectral resolution of 4 cm^{-1} and the scanning range of 4000 cm^{-1} to 500 cm^{-1} at room temperature. The crystallizations were characterized through X-ray diffraction (XRD, X'Pert Powder, Malvern Panalytical, The Netherlands) with the step size 2θ of 0.033° and the scanning range 2θ of 5° to 70° at room temperature. The chemical cross-linking network structures were analyzed by low-field nuclear magnetic resonance (LF-NMR, VTMR20-010 V-T, Niumai Corporation, China). The glass transition temperatures were performed by differential scanning calorimeter (DSC, DSC 3+, Mettler Toledo, Switzerland) with nitrogen flow rate of 40 mL/min in the temperature range of − 100 to 80 °C, the samples of 10 mg were used, and the heating rate was 10 °C/min. Dynamic mechanical analysis (DMA, DMA/SDTA861e, Mettler Toledo, Switzerland) was performed by a large tension device at a frequency of 1 Hz, the temperature range was from − 100 to 80 °C with a heating rate 5 °C/min under a nitrogen atmosphere, and the dimensions of the specimens were 5.5 mm (length) × 4 mm (width) × 1.5 mm (thickness). The mechanical properties were tested by universal testing machine (AGS-J, Shimadzu, Japan) at a constant strain rate of 100 mm min^{-1}, and the dimensions of the dumb-bell shaped samples were 20 mm (neck area length) × 4 mm (width) × 2 mm

(thickness). The fractured morphologies were carried out on scanning electron microscopy (SEM, SU8020, Hitachi, Japan), and the fractured surfaces were sputtered with gold.

Results and discussion

Cross-linking network structures of HTPE/PCL binders

Physical cross-linking network structures of HTPE/PCL binders

Hydrogen bonding is the electrostatic interaction between a group with a strong positive charge in the molecule and a negatively charged group. In polyurethane binder, the imino group on hard segment is a positively charged proton donor; both the ether group on soft segment and the carbonyl group on hard segment are negatively charged as proton acceptors. The imino groups can form hydrogen bonds with the ether groups and carbonyl groups, respectively. FT-IR is a simple but powerful technique for the investigation of hydrogen bonds in polyurethane binder, so we used it for characterizing the H-bonded interactions of HTPE/PCL binders with different PCL mass contents at room temperature, and the results are shown in Fig. 1.

The infrared band at 3328 cm^{-1} is due to the stretching of imino group, the 1728 cm^{-1} band is caused by carbonyl group, and the ether group is at 1108 cm^{-1} in Fig. 1. The H-bonded interactions in the HTPE/PCL binder are mainly formed by the carbonyl groups and imino groups, and the imino groups and the ether groups [33]. This is clearly demonstrated in Fig. 1, where the three groups show well-defined absorption bands. For a better analysis, these three infrared bands were treated separately in Fig. 2.

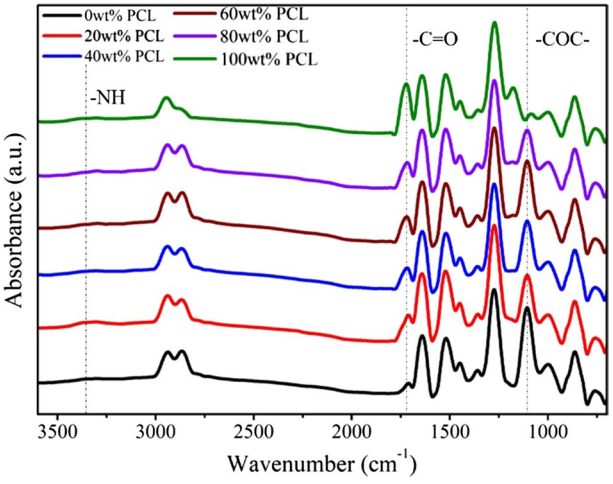

Fig. 1 The FT-IR spectra of HTPE/PCL binders

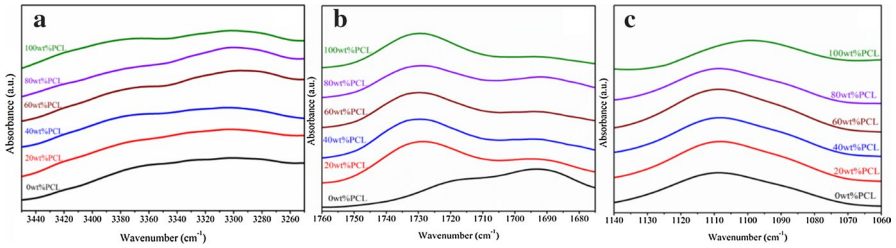

Fig. 2 The FT-IR spectra of HTPE/PCL binders, **a** the imino groups, **b** the carbonyl groups and **c** the ether groups

According to the FT-IR spectra in Fig. 2a, the infrared bands at 3380 cm^{-1} and 3300 cm^{-1} are due to the free imino stretching and ordered H-bonded imino stretching in HTPE/PCL binders with different PCL mass contents, respectively [34]. The binders in Fig. 2b involve two kinds of carbonyl groups; they are ordered carbonyl groups at the lower wavenumber that can form H-bonded interactions and the free carbonyl groups at the higher wavenumber [35]. The ether groups also present in ordered ether groups at the lower wavenumber and free ether groups at the higher wavenumber in Fig. 2c.

Because of the soft and hard segments of HTPE/PCL binder are thermodynamically incompatible or not completely compatible, the hard segments will agglomerate to produce microphase separation, facilitating the mechanical properties of the binder [36]. The stronger the hydrogen bond between the hard segments, the higher the microphase separation degree. On the contrary, the stronger the hydrogen bond formed through the hard and soft segments, the weaker the microphase separation degree. The microphase separation degree can be analyzed by different hydrogen bonds formed by the imino groups and the carbonyl groups, or by the imino groups and ether groups [37], and these two hydrogen bonds can also reflect the whole H-bonded interactions in HTPE/PCL binders. Therefore, further research on the FT-IR spectra of carbonyl and ether groups is needed.

However, the overlap of these ordered and free functional groups that obtained by FT-IR makes it hard to proceed further discussions. For distinguishing the overlapped carbonyl and ether groups, the second derivative of the FT-IR results was used to determine the accurate spectral absorption peaks of these different functional groups in HTPE/PCL binders, and the results are shown in Fig. 3. Figure 3a clearly demonstrates that the second derivative result of the carbonyl groups in HTPE/PCL binder has two peak valleys locating at 1731 cm^{-1} and 1690 cm^{-1}, which, respectively, correspond to free carbonyl groups and ordered H-bonded carbonyl groups. Figure 3b also shows the similar second derivative result, the free ether groups locate at 1111 cm^{-1}, and the ordered H-bonded ether groups are at 1088 cm^{-1}.

According to the numbers and locations of different carbonyl and ether groups in FT-IR spectra determined by second derivative, the multi-peak Gaussian fitting can be achieved to calculate the areas and proportions of these different functional groups in HTPE/PCL binders. Figure 4 is the multi-peak Gaussian fitting FT-IR spectra of carbonyl groups and ether groups (the uncertainty

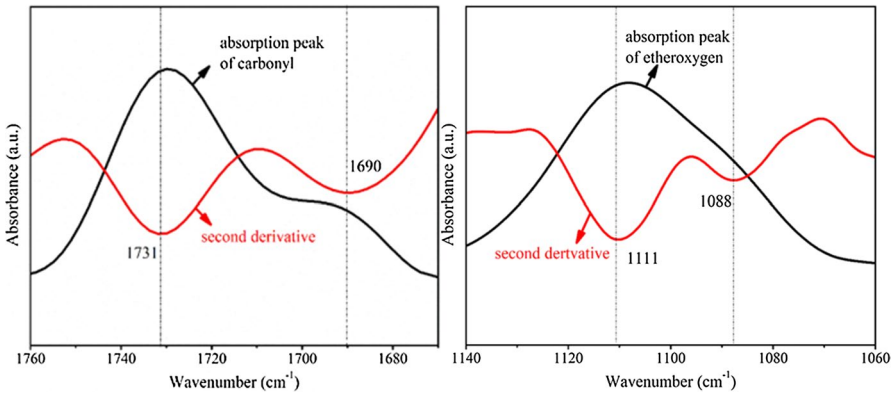

Fig. 3 The second derivative FT-IR spectra of HTPE/PCL binders, **a** the carbonyl groups and **b** the ether groups

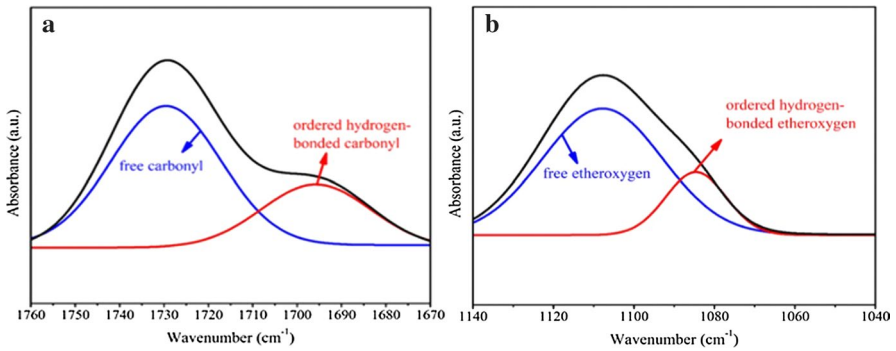

Fig. 4 The multi-peak Gaussian fitting FT-IR spectra of HTPE/PCL binders, **a** the carbonyl groups and **b** the ether groups

Table 1 The H-bond proportions of HTPE/PCL binders with different PCL mass contents

PCL content (wt%)	H–N…O=C X_H (%)	H–N…O–C X_H (%)	Total X_H (%)
0	45.88	8.17	54.05
20	45.93	8.63	54.56
40	43.97	14.21	58.18
60	41.96	19.61	61.57
80	38.34	20.06	58.40
100	32.58	10.43	43.01

R^2 associated with the fitting result of carbonyl group is more than 0.9966

R^2 associated with the fitting result of ether group is more than 0.9701

associated with the fitting result can be found in Supplementary Materials), and Table 1 is the obtained H-bond proportions in HTPE/PCL binders.

As shown in Table 1, the H-bond proportion formed by the carbonyl groups of HTPE/PCL binder decreases as the PCL mass content increases. After the introduction of PCL, its polar interaction leads to reduce the flexibility of the molecular chain and increase the distance between the hard segments. An increase in PCL mass content makes the molecular chain less flexible. More and more hard segments can evenly disperse in the soft segments, and the H-bonded interactions between hard segments are weakened. However, the carbonyl groups on the soft segments can also form H-bonded interactions with the imino groups on the hard segments. Thus, the H-bonded interactions formed by the carbonyl groups decrease slightly. It also proves that the degree of microphase separation in HTPE/PCL binder is reduced while enhancing PCL mass content. Because the H-bonded interactions formed by the ether groups on soft segments and imino groups on hard segments are increased from 8.17 to 20.06% when PCL mass content varied from 0 to 80 wt%. Enhancing the mass content of PCL can improve the compatibility of the soft and hard segments. After the hard segments evenly disperse in the soft segments, the probability of forming H-bond between the ether groups and the imino groups is raised. For the HTPE/PCL binders with PCL mass contents changed from 0 to 80 wt%, the reduction of H-bond proportions between the carbonyl groups and imino groups and the enhancement of H-bond proportions between the soft and hard segments make the H-bonded interactions have no obvious increase. But it can indicate that the microphase separation degree of the HTPE/PCL binders is declined. Moreover, because of the absence of HTPE, the reduction of ether group contents makes the H-bonded interactions formed by ether groups and the imino groups in the binder with 100 wt% PCL decrease.

Since the PCL prepolymer exhibits a semicrystalline state and the intermolecular interactions generated by crystallization will also form physical cross-linking network structures, XRD was used to verify the existence of crystal structure in the HTPE/PCL binders at room temperature. Figure 5 is the XRD patterns of HTPE/PCL binders with various PCL mass contents, and the inset figure in Fig. 5 is the XRD patterns of HTPE and PCL prepolymers. The XRD pattern of PCL prepolymer in the inset figure of Fig. 5 appears the crystal diffraction peak, indicating that crystallization occurs in PCL prepolymer. Moreover, all the XRD patterns of HTPE prepolymer and HTPE/PCL binders with different PCL mass contents are broad and amorphous diffraction peaks; it can be found that there is no crystal structure existing in HTPE prepolymer or in HTPE/PCL binders. This is due to N-100 as the curing agent has an average functionality of 3.87; the cross-linking network structures formed after HTPE/PCL binder completely curing destroy the original linear structures of HTPE and PCL. In addition, the small molecular Bu-NENA as the plasticizer also reduces the regularity of HTPE and PCL molecular chains. For these reasons, there is no intermolecular interaction generated by crystallization in the HTPE/PCL binders with different PCL mass contents at room temperature.

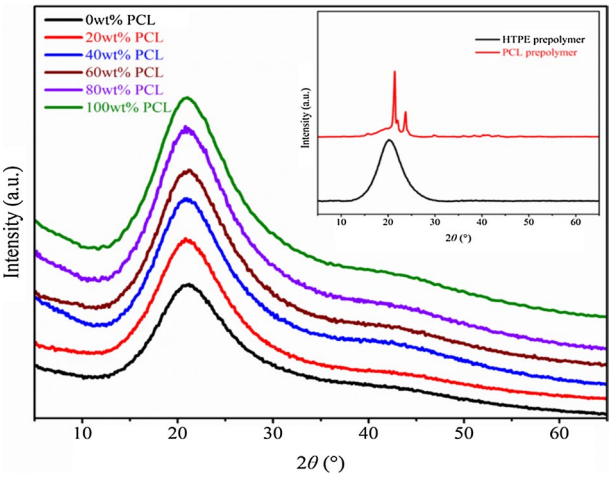

Fig. 5 The XRD patterns of HTPE/PCL binders with different PCL mass contents, and the inset is the XRD patterns of HTPE and PCL prepolymers

Chemical cross-linking network structures of HTPE/PCL binders

The chemical cross-linking network in HTPE/PCL binders can increase the interaction between the molecular chains and make them less prone to relative slippage. N-100 can be used as the chemical cross-linking point to form chemical cross-linking network in HTPE/PCL binder. The chemical cross-linking network structures of HTPE/PCL binders in diverse PCL mass contents were investigated by LF-NMR under the temperature range of 20 to 90 °C, and Eq. 1 is suitable for analyzing the cross-linking density (V_e) of the binders [38–40].

$$M(t) = Aexp\left(-\frac{t}{T_{21}} - \frac{qM_{rl}t^2}{2}\right) + Bexp\left(-\frac{t}{T_{22}}\right) + A_0 \quad (1)$$

where $M(t)$ is the attenuated signal; A and B denote the signal proportions of cross-linking and suspension chains, respectively; A_0 is the direct-current component; T_{21} and T_{22} are the relaxation times of cross-linking and related suspension chain signals, respectively; q is the anisotropy of the cross-linking chains; and M_{rl} represents the dipole moment below the glass transition temperature. Equation 1 was used to estimate these parameters, and V_e can be calculated by Eq. 2.

$$V_e = \frac{5\rho N\sqrt{qM_{rl}}}{3CM} \quad (2)$$

where ρ is the density of the binder; N is the bond number of the repeat unit on backbone chain; C represents the bond number in segment; and M is the molar mass of the repeat unit. The obtained results are shown in Table 2 including the V_e and the molecular weight between the cross-linking points (M_c) of the binders.

Table 2 The chemical cross-linking network parameters of the HTPEPCL binders with diverse PCL mass contents

PCL content (wt%)	20 °C		50 °C		70 °C		90 °C	
	$V_e \times 10^{-4}$ (mol cm^{-3})	$M_c \times 10^3$ (g mol^{-1})	$V_e \times 10^{-4}$ (mol cm^{-3})	$M_c \times 10^3$ (g mol^{-1})	$V_e \times 10^{-4}$ (mol cm^{-3})	$M_c \times 10^3$ (g mol^{-1})	$V_e \times 10^{-4}$ (mol cm^{-3})	$M_c \times 10^3$ (g mol^{-1})
0	3.489	2.866	2.756	3.628	2.574	3.924	2.033	4.919
20	3.741	2.673	2.874	3.479	2.649	3.775	2.148	4.655
40	3.862	2.590	3.210	3.115	2.804	3.566	2.429	4.117
60	4.255	2.350	3.419	2.925	2.992	3.342	2.658	3.762
80	4.244	2.357	3.643	2.744	3.107	3.218	2.838	3.524
100	4.397	2.274	3.852	2.596	3.387	2.953	3.096	3.230

The stander deviation (StDev) associated with V_e at 20 °C, 50 °C, 70 °C and 90 °C is less than 0.208, 0.828, 0.187 and 0.377, respectively

The StDev associated with M_c at 20 °C, 50 °C, 70 °C and 90 °C is less than 0.189, 0.189, 0.607 and 0.185, respectively

In the same temperature, Table 2 clearly demonstrates that the V_e of HTPE/PCL binder enhances with the increase in PCL mass content, but the M_c continues to decrease. The introduction of PCL with a lower molecular weight can increase the relative concentration of hydroxyl groups before the curing reaction, so the probability of PCL entering the cross-linking network of the HTPE/PCL binder increases and the V_e was enhanced after the curing reaction. However, the improved V_e of HTPE/PCL binder can also increase the intertwining of the molecular chains and the ability of cross-linking point to limit the activity of the molecular chains. These factors lead to a decreasing tendency in the mobility of the HTPE and PCL molecular chains; the molecular chains are hard to be extended further. Thus, the M_c of HTPE/PCL binder is lowered under the same temperature. In addition, at the same mass content of PCL, the temperature has a great influence on the physical cross-linking network structures formed by H-bonded interactions of the HTPE/PCL binder. When the temperature increases, the H-boned interaction is weakened, the physical cross-linking network is broken, and the interaction between the molecular chains is reduced. For these reasons, the V_e of the HTPE/PCL binders is lowered and the M_c is enhanced when the temperature raises.

Integrity of cross-linking network structures

Cross-linking network structures are the microstructural factors of HTPE/PCL binders, and these factors affect the network structures in different ways. Evaluating the cross-linking network structures synthetically and reflecting the mechanical properties from the perspective of the network structures are issues that need to be studied deeply. Therefore, the degree of integrity of HTPE/PCL binder network was studied by comparing the calculated and actual elastic modulus according to the rubber elasticity statistical theory of cross-linking structure [41]. All the work done by the external force on the binder is converted to the stored energy of the elastomer, and the energy function is

$$w = \frac{G(\lambda_1^2 + \lambda_2^2 + \lambda_3^2 - 3)}{2} \tag{3}$$

where λ is Poisson ratio, dimensionless; G is the shear modulus of binder, MPa.

The shear modulus (G) and the cross-linking network parameters have the following interrelations:

$$G = NkT = \frac{N_A \rho kT}{M_C} = \frac{\rho RT}{M_C} \tag{4}$$

where N is the total chain number in the cross-linking network; k is the Boltzmann constant; T is the absolute temperature; K N_A is the Avogadro constant; ρ is the density of binder, g cm^{-3}; and R is the molar gas constant.

The rubber elasticity statistical theory of cross-linking structure assumes that the ends of each chain in the cross-linking network are connected to the cross-linking point, and all the chains contribute to the modulus, which is an idealized case. But it is impossible to be so ideal in the cross-linking network structure, because multiple

structural defects exist, like physical entanglements, enclosed rings, pendant groups and free chains on the molecular chains. Except the entanglements, the enclosed rings, pendant groups and free chains have adverse influence on the mechanical property of the binder, so it is hard to calculate and count the exact defects and their interactions. To reflect the integrity of cross-linking network structure of HTPE/PCL binder, a correction factor (D) was introducing into Eq. 4, and D is used to indicate the contribution of the defects and their interactions to G, so Eq. 4 can be rewritten as:

$$G = \frac{\rho RT}{M_C} + D \tag{5}$$

When the elongation is very small, G and elastic modulus (E) have a relationship of $E = 3G$; thus, Eq. 5 can be changed into:

$$E = \frac{3\rho RT}{M_C} + 3D \tag{6}$$

The correction factor D indicates the relative contributions of H-bonded interactions and defects to the modulus of HTPE/PCL binder. The positive value of correction factor D is on behalf of the influence of H-bonded interactions on the modulus of binder is more effective than that of the defects, presenting that the cross-linking network structures of the binder possess a better integrity, or vice versa. The results of correction factor D of HTPE/PCL binders at room temperature are shown in Table 3 for a further analysis.

As the results in Table 3, the correction factors D of HTPE/PCL binders are all negative values, indicating that the cross-linking network structures of binders have defects. Nevertheless, the relatively superior network structure, which has the maximal correction factor, might be selected for application. Correction factor D increased from −0.76 to −0.64 within the PCL content of 0 wt% to 40 wt%. The introduction of PCL with a lower molecular weight than HTPE can increase the relative concentration of hydroxyl groups before the curing reaction, which is beneficial to increase the curing conversion rate. It can enhance the physical entanglements and reduce the probabilities of defects such as enclosed rings, pendant groups

Table 3 The cross-linking network integrity of the HTPE/PCL binders

PCL content (wt%)	E (MPa)	ρ (g cm^{-3})	$M_c \times 10^3$ (g mol^{-1})	D
0	0.13	0.93	2.866	− 0.76
20	0.35	0.93	2.673	− 0.74
40	0.72	0.92	2.590	− 0.64
60	0.70	0.93	2.350	− 0.75
80	0.72	0.91	2.357	− 0.72
100	0.49	0.92	2.274	− 0.84

The StDev associated with D is less than 0.61×10^{-2}

and free chains after curing, so the cross-linking network structures of the binders are gradually improved. However, when PCL content exceeds 40 wt%, as the degree of microphase separation of HTPE binder continues to decrease, the micro-interval cohesions between the hard segments decrease, which will destroy the integrity of the network structure. Therefore, the correction factor *D* has a declined trend when PCL content increases after 40 wt%.

Thermal properties of HTPE/PCL binders

Figure 6 shows the DSC curves of HTPE/PCL binders with different PCL mass contents. The glass transition temperature (T_g) values of HTPE binder (0 wt% PCL) and PCL binder (100 wt% PCL) in Fig. 6 are found to be −76.89 and −73.91 °C, respectively. With the increase in mass content of PCL, the DSC curves show that only one T_g of each binder is observed, which is located in between the T_g of HTPE binder and PCL binder, respectively. It indicates that the motion of soft segments is affected by the cross-linking networks in HTPE/PCL binders. This phenomenon is ascribed to the fact that the HTPE and PCL components both are relatively long molecular chains, and some fractions of soft segments close to polyurethane hard segments located at the ends of HTPE or PCL molecular chains are restricted by the cross-linking networks and the gaps between cross-linking points [42].

The loss factor (tan δ) versus temperature of HTPE/PCL binders from DMA is shown in Fig. 7. Comparing with the regional scale motion of polymer segments revealed by glass transition from DSC, DMA is a sensitive technique for studying the initial motion of polymer segment by α relaxation at molecular scale [43]. All the HTPE/PCL binders with different PCL mass contents show one region of mechanical loss; the α relaxation temperature (T_α) of HTPE/PCL binder gradually increases from −73.77 to −55.02 °C with adding PCL. T_α is associated with the coordinated movements of soft and hard segments of polymer chains in HTPE/PCL

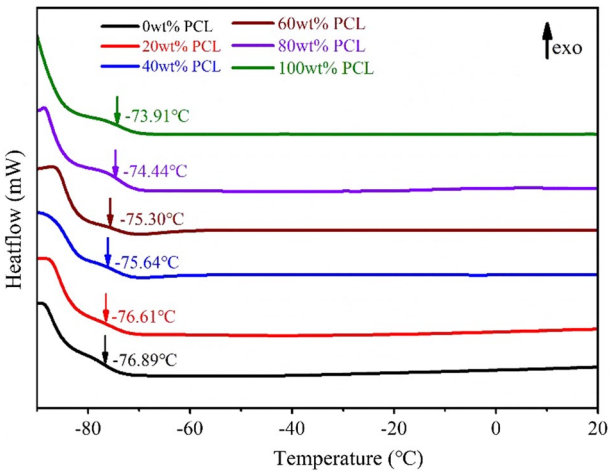

Fig. 6 The DSC curves of HTPE/PCL binders with different PCL mass contents

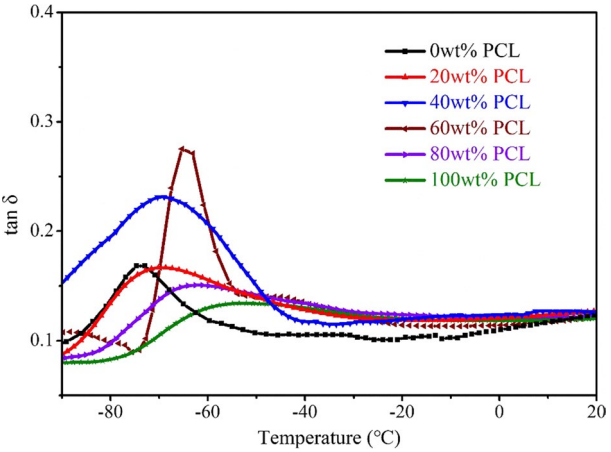

Fig. 7 The tan δ-temperature curves for HTPE/PCL binders with different PCL mass contents

binder. The increasing trend of T_α is agreement with that of the H-bonded interaction and the cross-linking density of HTPE/PCL binder. The change of T_α comes from the entanglements among the polymer chains of the cross-linking networks. The increasing trend of T_α of HTPE/PCL binder reveals that the inhibition of cross-linking network on polymer chains motion is enhanced with the increase in PCL mass content.

Mechanical properties of HTPE/PCL binders

In order to analyze the mechanical properties of HTPE/PCL binders under the wide temperature range of − 50–70 °C, a universal testing machine was used to characterized the mechanical properties of the binders with different PCL mass contents. The corresponding results of maximum tensile strength (σ_m) and elongation at break (ε_b) are shown in Table 4, and the stress–strain curves are shown in Fig. 8. The increase in H-bonded interaction and cross-linking density of the binder can enhance its interaction between molecular chains. The molecular chain is hardly prone to relative slippage, which can improve the mechanical property of the binder. In addition, the mechanical strength of the binder can also be enhanced by increasing the degree of microphase separation.

By integrating the stress–strain curves of HTPE/PCL binders under different temperatures, the integral values ($\int \sigma d\varepsilon$) can reflect the toughness of the binders [44]. The larger the integral value, the tougher the HTPE/PCL binder is. According to the mechanical properties,

$$\sigma = \frac{F}{S} \tag{7}$$

Table 4 The σ_m and ε_b of HTPE/PCL binders under wide temperature range

PCL content (wt%)	−50 °C		−40 °C		20 °C		50 °C		70 °C	
	σ_m (MPa)	ε_b (%)	σ_m (MPa)	ε_b (%)	σ_m (MPa)	ε_b (%)	σ_m (MPa)	ε_b (%)	σ_m (MPa)	ε_b (%)
0	1.64	346.34	1.32	351.97	0.63	85.98	0.61	82.36	0.57	78.79
20	1.69	335.26	1.41	344.01	0.64	82.85	0.61	74.94	0.58	71.46
40	3.06	352.16	2.69	370.99	0.81	76.00	0.74	59.81	0.68	51.93
60	3.58	399.51	3.01	424.03	0.71	71.65	0.68	56.04	0.65	46.79
80	4.99	410.40	4.69	432.96	0.67	52.77	0.61	47.81	0.59	46.91
100	5.09	460.74	5.03	468.98	0.52	50.97	0.33	34.69	0.21	24.42

The StDev associated with σ_m at −50 °C, −40 °C, 20 °C, 50 °C and 70 °C is less than 0.55, 0.54, 0.09, 0.09 and 0.23, respectively

The StDev associated with ε_b at −50 °C, −40 °C, 20 °C, 50 °C and 70 °C is less than 23.87, 22.79, 8.04, 4.39 and 5.52, respectively

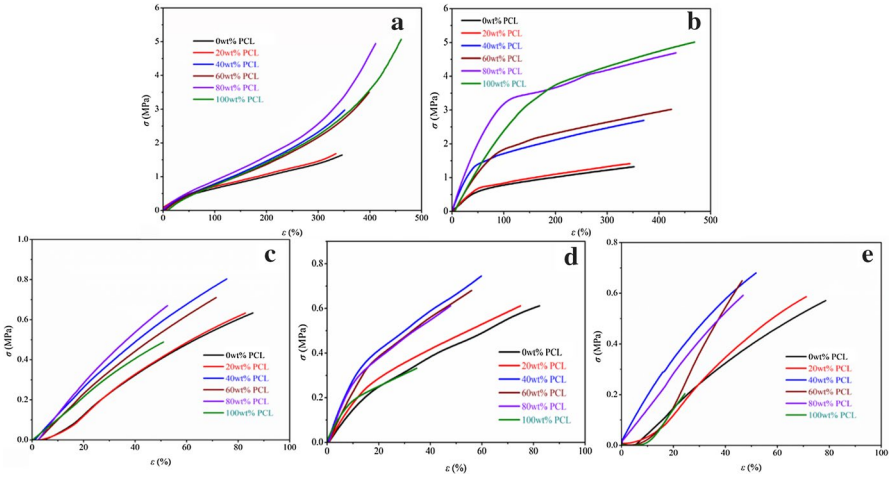

Fig. 8 The stress–strain curves of HTPE/PCL binders, **a** − 50 °C, **b** − 40 °C, **c** 20 °C, **d** 50 °C and **e** 70 °C

$$\varepsilon = \frac{L}{L_0} \tag{8}$$

$$\int \sigma \mathrm{d}\varepsilon = \frac{1}{L_0} \times \int \left(\frac{F}{S}\right) \mathrm{d}L \tag{9}$$

$$W = \int F \mathrm{d}L \tag{10}$$

where F is the tensile force, N; S is the cross-sectional area, m^2; L is the extension length, m; L_0 is the original length of the sample, m; and W is the work until fracture, J. Assuming that the cross-sectional area of the binder is constant during the stretching process, the integral values can be regarded as the work done by the force F until fracture, which is fracture work. The fracture work is affected significantly by either strength or elongation. Figure 9 is the fracture works of HTPE/PCL binders under the wide temperature range of − 50–70 °C.

Mechanical properties of HTPE/PCL binders at room temperature

According to the observations from Table 4 and Fig. 8c, with the augment of PCL content, the maximum tensile strength of HTPE/PCL binder increases when PCL content does not exceed 40 wt%. Otherwise, the maximum tensile strength begins to decline. When the PCL content is 40 wt%, the HTPE/PCL binder can obtain the better maximum tensile strength and fracture work, which are 0.81 MPa and 1.84 J, respectively. But, its elongation at break continuously decreases from 85.98 to 50.97%.

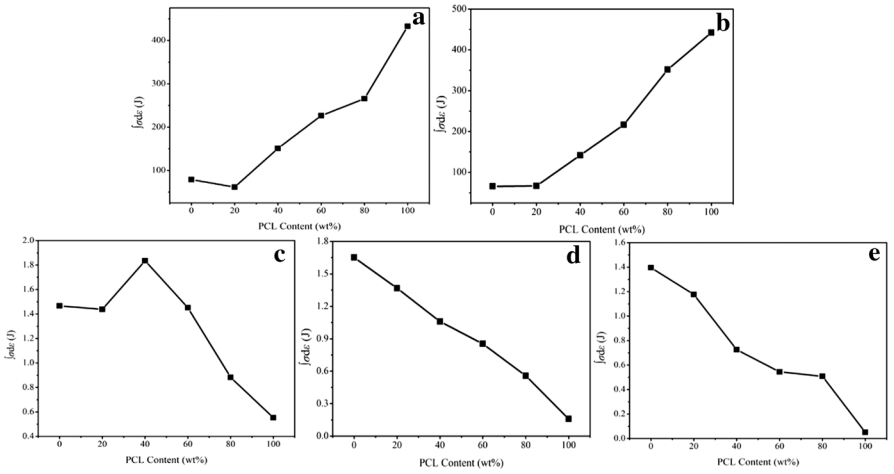

Fig. 9 The fracture work of HTPE/PCL binders, **a** − 50 °C, **b** − 40 °C, **c** 20 °C, **d** 50 °C, and **e** 70 °C

Through the above analysis, it is found that the H-bonded interaction of HTPE/PCL binder is not significantly affected by the continuous addition of PCL. Although its cross-linking density sustains to increase, the microphase separation degree continuously reduces. When the addition amount of PCL does not exceed 40 wt%, the contribution of the increase in the cross-linking density of the HTPE/PCL binder to its strength can offset the impact of the decrease in the microphase separation degree on the strength, and the integrity of the network structures is improved, so the maximum tensile strength of the binder has seen an improvement at this time. The enhanced chemical network structures and strength also make the fracture work increase before the PCL content is 40 wt%. However, after the addition content of PCL exceeding 40 wt%, the degree of microphase separation of the HTPE/PCL binder continuously reduces, resulting in a decline in micro-interval cohesion in the hard segment; this will destroy the integrity of the cross-linking network structure. At this point, the increase in cross-linking density cannot offset the reduction of microphase separation degree on the strength of binder, and the maximum tensile strength of HTPE/PCL binder begins to reduce.

Besides, the enhancement of cross-linking effect will affect the flexibility of the molecular chain, the activity ability of molecular chain is weakened, and it is difficult to achieve a further extension for the molecular chain. Moreover, the molecular weight between the cross-linking points and the microphase separation degree are both reduced. All these factors together lead to the elongation at break, and the fracture work of HTPE/PCL binder decreases as the PCL mass content increases.

Mechanical properties of HTPE/PCL binders at high temperature

According to the stress–strain curves at high temperatures (50 °C and 70 °C) in Fig. 8d, e, and their results in Table 4, the maximum tensile strength of HTPE/PCL binder at 50 °C is enhanced at the beginning of adding PCL, and then, it goes down

with further adding PCL. The maximum tensile strength at 70 °C also shows the same trend. When the addition amount of PCL is 40 wt%, the maximum tensile strength of the binder at high temperature comes to the largest value, which achieves to 0.74 MPa at 50 °C and 0.68 MPa at 70 °C, respectively. And the elongation at break of HTPE/PCL binder declines continuously. However, the fracture work of the binder under high temperature continues to decrease when the PCL increases.

Comparing with the mechanical properties of the binders at 20 °C, the hydrogen bond in HTPE/PCL binder is broken due to the rise in temperature, weakening the H-bonded interaction. At the same time, the constrain between molecular chains decreases, and the enhancement of molecular chain activity enables the hard segment to disperse evenly in the soft segment. As thus, the enhancements in isolating, shielding and coupling between these molecular chains lead to a decline in the physical cross-linking density and a weakening of microphase separation degree [45]. Therefore, the mechanical properties of HTPE/PCL binders in different PCL mass contents at high temperature are lower than those at room temperature. At the same time, due to the destruction of the cross-linking network structures, the reduction of strength and elongation lead to a decreasing trend in fracture work.

Mechanical properties of HTPE/PCL binders at low temperature

On the basis of Table 4 and Fig. 8a, b, the maximum tensile strengthens of HTPE/PCL binders at −50 °C and −40 °C both demonstrate the increasing tendency with the addition of PCL, but the elongation at break reaches their minimum values when PCL content is 20 wt%, which are 344.01% at −40 °C and 335.26% at −50 °C, respectively. The fracture works at low temperature show the same trend with the elongation at break.

Comparing with that at 20 °C, the mechanical properties at low temperature are greatly improved. The curing reaction destroys the normal linear structure of HTPE and PCL, and the addition of Bu-NENA as the small molecular plasticizer also increases the distances between the molecular chains. When the temperature decreases to −40 °C or −50 °C, the lower temperature and the applied stress lead to an improvement of the orientation of the molecular chains, and their arrangement becomes regular. In this way, the ordered regions formed by the soft and hard segments in HTPE/PCL binder can be further nucleated, and the orientational induction promotes crystallization. Therefore, the strain-induced crystals appear in the HTPE/PCL binder during the stretching process at the low temperature [46]. After crystallization, the molecular segment of HTPE/PCL binder becomes more regular, and the interaction between the soft and hard segments is enhanced; these reasons are the facts for improving the strength of HTPE/PCL binder.

Due to the occurrence of strain-induced crystallization, the hard segment microregions in HTPE binder aggregate and the soft segments are more likely to gather together, which can improve the flexibility of the polymer segments, and thus, the elongation at break has been enhanced. In the process of adding PCL, the elongation at break of HTPE/PCL binder demonstrates a tendency to decrease first and then increase. This is because the HTPE molecular chain is more flexible than the PCL molecular chain, and a little addition amount of PCL with strong polar effect

will reduce the flexibility of the original HTPE molecular chain, so the elongation at break of HTPE/PCL binder is declined and the fracture work slightly reduces at the beginning of adding PCL. However, with the increasing content of PCL, its polar effect makes the PCL molecular chains more likely to gather around, it can improve the orientation of the molecular chains, and the effect of strain-induced crystallization of the binder is enhanced. Therefore, the elongation at break and the fracture work of HTPE/PCL binder have improved when the addition amount of PCL exceeds 20 wt%. The activity of molecular chain in the binder at − 50 °C is more restricted than that at − 40 °C, so the elongation at break of the binder at − 40 °C is higher than it at − 50 °C.

Fractured morphologies of HTPE/PCL binders

Figure 10 is the morphological characteristics of the fractured surfaces of HTPE/PCL binders with 40 wt% PCL under the wide temperature range of − 50–70 °C (the other fractured surfaces of HTPE/PCL binders are shown in Supplementary Materials). It can be observed from Fig. 10 that there is no obvious phase separation existing in HTPE/PCL binder under different temperatures. The homogeneous surfaces of the binders indicate that the polymer chains penetrate inward and outward in the cross-linking network structures showing the good compatibility of HTPE and PCL.

Cracks will appear in the HTPE/PCL binder due to the stress concentration while stretching. Then, the cracks grow in the binder as the stretch progressing, eventually causing the binder to break. At the low temperature, the cracks in Fig. 10a, b are few and the fractured surfaces of HTPE/PCL binders are rough, which indicate that the interaction between the polymer segments is enhanced and the crack is hard to grow. With the increase in temperatures, the further destruction to the cross-linking network structures and the decrease in constrain between molecular chains lead to the

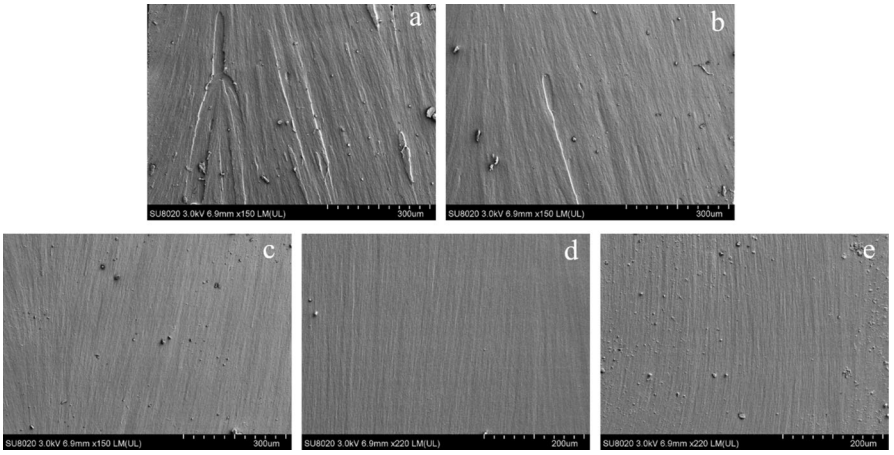

Fig. 10 The SEM images for the fractured surface of HTPE/PCL binder with 40 wt% PCL, **a** − 50 °C, **b** − 40 °C, **c** 20 °C, **d** 50 °C and **e** 70 °C

easier growth of cracks in the binder; thus, the fractured surfaces gradually become smooth and the cracks increase.

Conclusions

In this work, a series of polyurethane binders based on HTPE and PCL were prepared. The mechanical properties of HTPE/PCL binders in the wide temperature range of − 50–70 °C can be regulated by changing the mass ratios of HTPE versus PCL. The cross-linking network structures in the binders determine the mechanical properties. The changes in PCL mass contents have no obvious influence on H-bonded interactions in HTPE/PCL binders, but the enhancement of PCL mass content reduces their microphase separation degrees. PCL is found to improve the cross-linking density of HTPE/PCL binder more than HTPE. However, the cross-linking density reduces due to the physical interactions being broken in higher temperature. The cross-linking network structures destroy the linear regularity structures of original molecular chains; thus, there are no obvious crystal structures of HTPE/PCL binders at room temperature. It is found that the HTPE/PCL binder can possess the better cross-linking network structures and mechanical properties under the wide temperature range when the PCL mass content is 40 wt% by comparison. Strain-induced crystallization improves the low-temperature mechanical properties of the binder, but the reduced cross-linking density and microphase separation degree in turn decrease their mechanical properties in high temperature. These results of this study prove that the introduction of PCL can improve the mechanical properties of original HTPE binder, and the HTPE/PCL binder with 40 wt% PCL is suitable for the future investigation of HTPE/PCL propellants.

References

1. Tan HM (2015) The chemistry and technology of solid rocket propellant, 1st edn. Beijing Institute of Technology Press, Beijing, p 186
2. Duncan ES, Margetson J (2009) A nonlinear viscoelastic theory for solid rocket propellants based on a cumulative damage approach. Propell Explos Pyrot 23:94–104
3. Li G, Wang Y, Jiang A, Yang M (2018) Micromechanical investigation of debonding processes in composite solid propellants. Propell Explos Pyrot 43:642–649
4. Zhang L, Zhi S, Shen Z (2018) Research on tensile mechanical properties and damage mechanism of composite solid propellants. Propell Explos Pyrot 43:234–240
5. Bhowmik D, Sadavarte VS, Pande SM, Saraswat BS (2015) An energetic binder for the formulation of advanced solid rocket propellants. Cent Eur J Energ Mater 12:145–158
6. Colclough ME, Desai H, Millar RW, Paul NC, Stewart MJ, Golding P (1994) Energetic polymers as binders in composite propellants and explosives. Polym Adv Technol 5:554–560
7. Davenas A (2003) Development of modern solid propellants. J Propul Power 19:1108–1128
8. Li Y, Li J, Ma S, Luo YJ (2016) Different catalytic systems on hydroxyl-terminated GAP and PET with poly-isocyanate: curing kinetics study using dynamic in situ IR spectroscopy. Int J Polym Anal Charact 21:495–503
9. Manu SK, Varghese TL, Mathew S, Ninan KN (2010) Studies on structure property correlation of cross-linked glycidyl azide polymer. J Appl Polym Sci 114:3360–3368
10. Luo YJ, Wang XQ, Ge Z (2011) Energetic polymers, 1st edn. National Defense Industry Press, Beijing, pp 144–145

11. Coleman MM, Lee KH, Skrovanek DJ, Painter PC (1986) Hydrogen bonding in polymers. 4. Infrared temperature studies of a simple polyurethane. Macromolecules 19:2149–2157
12. Luo N, Wang D, Ying SK (1997) Hydrogen-bonding properties of segmented polyether poly(urethane urea) copolymer. Macromolecules 30:4405–4409
13. Yarmohammadi M, Komeili S, Shahidzadeh M (2018) Studying crosslinker chemical structure effect on the tuning properties of HTPB-based polyurethane. Propell Explos Pyrot 43:156–161
14. Ou YP, Sun Y, Jiao Q (2018) Properties related to linear and branched network structure of hydroxyl terminated polybutadiene. e-Polymers 18:267–274
15. Xia M, Luo YJ, Mao KZ (2014) The Mechanism of thermal decomposition of HTPE binder and its effect on the thermal decomposition characteristics of AP. China Academic Journal Electronic Publishing House. http://cpfd.cnki.com.cn/Article/CPFDTOTAL-HNCL201411001069.htm. Accessed 21 Nov 2014
16. Wang G, Fan WW, Zhang X, Zhang WB, Zhu XZ, Fan XD (2015) Synthesis of poly(ethylene oxide)-poly(tetrahydrofuran) diblock copolymer by end group protection. Polym Mater Sci Eng 31:27–30
17. Wang CD, Luo YJ, Xia M (2011) Synthesis of HTPE and properties of HTPE elastomers. Chin J Energ Mater 19:518–522
18. Kai F, Tokerud D,Biserod H, Orbekk E, Tenden S, Kaiserman M, Rodack M, Spate W, Winetrobe S, Royce B, Wallace S (2005) The hypervelocity anti-tank missile development program: rocket motor design and development. American Institute of Aeronautics and Astronautics Press. https://doi.org/10.2514/6.2005-4172. Accessed 19 June 2012
19. Kaiserman M, Rodack M, Spate W, Winetrobe S, Royce B, Wallace S, Biserod H, Fossumstuen K, Tokerud D (2005) An overview of the hypervelocity anti-tank missile (HATM) development program. American Institute of Aeronautics and Astronautics Press. https://doi.org/10.2514/6.2005-4171. Accessed 19 June 2012
20. Song XQ, Zhou JY, Wang WH, Li XH (2008) Review on HTPE propellants. Chin J Energ Mater 16:349–352
21. Liao LQ, Xu HX, Li YH, Pang WQ, Zhang NN, Wang JL, Liu GL (2010) Experimental study on hazard of HTPB propellants. Chin J Explos Propell 33:28–31
22. Yan DQ, Xu DD, Shi JG (2009) A review of solid propellant binder HTPE development and its molecular design philosophy. J Solid Rocket Technol 32:644–649
23. Zhang QF, Zhang JQ (2004) Research and development of insensitive solid propellants. Chin J Energ Mater 12:371–375
24. Mao KZ, Xia M, Luo YJ, Zhang ZJ (2012) Effect of curing agent types on properties of HTPE polyurethane elastomer films. Chin J Explos Propell 35:55–58
25. Millar RW, Philbin SP, Claridge RP, Hamid J (2010) Studies of novel heterocyclic insensitive high explosive compounds: pyridines, pyrimidines, pyrazines and their bicyclic analogues. Propell Explos Pyrot 29:81–92
26. Pagoria PF, Lee GS, Mitchell AR, Schmidt RD (2002) A review of energetic materials synthesis. Thermochimica Acta 384(1):187–204
27. Pang AM, Zheng J (2004) Prospect of the research and development of high energy solid propellant technology. J Solid Rocket Technol 27(4):289–293
28. Brunette CM, Hsu SL, Macknight WJ (1982) Hydrogen-bonding properties of hard-segment model compounds in polyurethane block copolymers. Macromolecule 15:71–77
29. Wang Y, Dang H, Zeng H, Bai J, Lei Y, Liu L, Li Z (2016) Properties of PCL/MDI/BDO polyurethane elastomer. Plastics 6:93–95
30. Wang X, Zhao H, Turng L-S, Qian L (2013) Crystalline morphology of electrospun poly(ε-caprolactone) (PCL) nanofibers. Ind Eng Chem Res 52:4939–4949
31. Min BS, Ko SW (2013) Characterization of segmented block copolyurethane network based on glycidyl azide polymer and polycaprolactone. Macromol Res 15:225–233
32. Min BS (2008) Characterization of the plasticized GAP/PEG and GAP/PCL block copolyurethane binder matrices and its propellants. Propell Explos Pyrot 33:131–138
33. Yilgor I, Yilgor E, Guler IG, Ward TC, Wilkes GL (2006) FTIR investigation of the influence of diisocyanate symmetry on the morphology development in model segmented polyurethanes. Polymer 47:4105–4114
34. Tien YI, Wei KH (2001) Hydrogen bonding and mechanical properties in segmented montmorillonite/polyurethane nanocomposites of different hard segment ratios. Polymer 42:3213–3221

35. Ma S, Li YJ, Li GP, Luo YJ (2017) Research on the mechanical properties and curing networks of energetic GAP/TDI binders. Cent Eur J Energ Mater 14:708–725
36. Chen ZS (1990) Study on properties and phase separation of segmented polyurea for different hard segment content. Polym Mater Sci Eng 3:26–31
37. Chen XD, Zhou NQ, Zhang H, Zhou CH, Chen RS (2008) Characterization methods for polyurethane elastomer micro-phase separated structure. Chi Elastom 18:58–65
38. Garbarczyk M, Grinberg F, Nestle N, Kuhn W (2001) A novel approach to the determination of the crosslink density in rubber materials with the dipolar correlation effect in low magnetic fields. J Polym Sci Polym Phys 39:2207–2216
39. Kuhn W, Theis I, Koeller E (1991) Network dynamics of crosslinked polymers-crosslinking, filler and aging characterized by NMR parameters. Mater Res Soc Symp Proc 33:217–223
40. Azoug A, Constantinescu A, Nevière R, Jacob G (2015) Microstructure and deformation mechanisms of a solid propellant using ^{1}H NMR spectroscopy. Fuel 148:39–47
41. Fried E (2002) An elementary molecular-statistical basis for the Mooney and Rivlin–Saunders theories of rubber elasticity. J Mech Phys Solids 50:571–582
42. Li YJ, Li J, Ma S, Luo YJ (2017) Compatibility, mechanical and thermal properties of GAP/P(EO-*co*-THF) blends obtained upon a urethane-curing reaction. Polym Bull 74:4607–4618
43. Ding YZ, Hu C, Guo X, Che YY, Huang J (2014) Structure and mechanical properties of novel composites based on glycidyl azide polymer and propargyl-terminated polybutadiene as potential binder of solid propellant. J Appl Polym Sci 137:1–8
44. Tattersall HG, Tappin G (1966) The work of fracture and its measurement in metals, ceramics and other materials. J Mater Sci 1:296–301
45. Mao KZ, Ma S, Luo YJ (2016) Effect of TDI on the mechanical property and crosslinking network structure integrity. J Solid Rocket Technol 3:378–382
46. Chen Y, Zhang H, Fang X, Lin Y, Xu Y, Weng W (2014) Mechanical activation of mechanophore enhanced by strong hydrogen bonding interactions. Acs Macro Lett 3:141–145